ChemComm

Accepted Manuscript

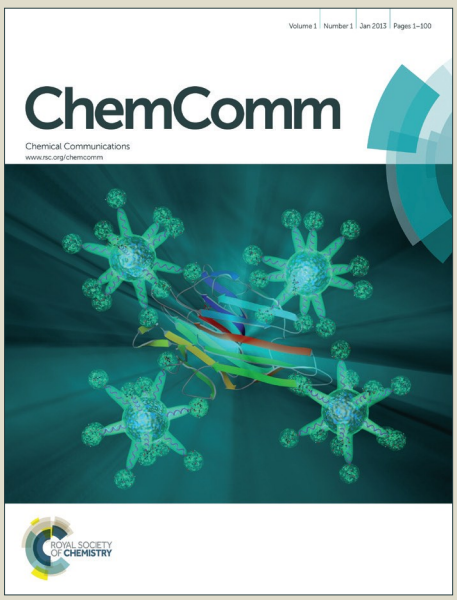

ROYAL SOCIETY OF CHEMISTRY

www.rsc.org/chemcomm

Journal Name

COMMUNICATION

Reprogrammable Multiplexed Detection of Circulating OncomiRs Using Hybridization Chain Reaction

Received 00th January 20xx,
Accepted 00th January 20xx

DOI: 10.1039/x0xx00000x

www.rsc.org/

Muhit Rana[a], Mustafa Balcioglu[a], Maya Kovach[a], Mustafa Salih Hizir[a], Neil M. Robertson[a], Irfan Khan[a, b] and Mehmet V. Yigit [a, b, *]

In this study, we have coupled the DNA polymerization capability of hybridization chain reaction (HCR) with the plasmonic properties of gold nanoparticles to develop a reprogrammable and multiplexed detection of three circulating oncomiRs (miR-10b, miR-21 and miR-141) dysregulated in various disease states of breast cancer. We have demonstrated that by simply changing the initiator (label-free short single stranded DNA) content of the HCR, while keeping everything else unchanged, the same nanoparticle assembly can be reprogrammed for the detection of the target oncomiRs individually or simultaneously in all possible combinations. We have shown that as little as 20 femtomole of each oncomiR can be detected visually without using any analytical instrument. Furthermore, we demonstrated that the target oncomiR can be detected in an RNA pool isolated from a liquid biopsy mimic of breast cancer.

DNA nanotechnology has advanced remarkably over the last decade offering a wide range of applications for biomedical and fundamental research.[1-3] One of the highly powerful developments in DNA nanotechnology is the hybridization chain reaction (HCR) discovered by Pierce and coworkers.[4] In HCR, two kinetically trapped metastable hairpin DNAs (H1 and H2) do not hybridize to each other when present together, however have a strong potential to form a long chain of DNA polymers with an external stimulus. The addition of a short single stranded (ss) DNA (initiator) binds, opens, and activates the first hairpin (H1, **scheme 1-I**) which immediately hybridizes with, and opens the second hairpin (H2, **scheme 1-II**). The opening of H2 forms a nicked double strand, which induces the opening of another H1, and the hybridization chain reaction occurs, **scheme 1-III**. As a result, long double stranded DNA polymers assemble from H1 and H2 (**scheme 1-IV)**, which was unable happen in the absence of an initiator strand. This powerful technology has resulted in developing methodologies for the detection of mRNAs inside live cells and higher organisms.[5-7] Others have used this technology for chemo-drug delivery for cancer theranostics[8, 9] and detection of short DNA strands.[10, 11] Here, we have used this technology to develop a reprogrammable RNA detection methodology, which offers individual and simultaneous detection of three different circulating miRNAs.

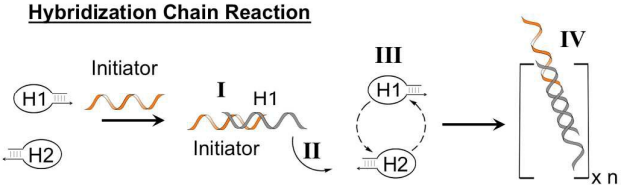

Scheme 1. Schematic illustration of the hybridization chain reaction.

miRNAs are small non-coding RNA molecules (22-23 nts) which regulate gene expression by translational repression or mRNA degradation. A number of miRNAs are linked to many types of cancer, referred to as oncomiRs, and found to be dysregulated in the solid and liquid biopsies of cancer patients.[12] Abnormal expression levels of oncomiRs are observed at different stages of oncogenesis, reflect the physiological state of cancer and can be used for the diagnosis and prognosis of the disease.[13-15] For instance, miR-10b is over-expressed in metastatic breast cancer and its expression is correlated with the aggressiveness of the disease.[16, 17] On the other hand, miR-21 is dysregulated in drug-resistant phenotypes of breast cancer[18, 19] and miR-141 is found to be significantly upregulated in the specimens of breast cancer patients with stage I-III and lymph node metastasis.[20] The findings, along with many others, demonstrate that the expression of oncomiRs varies at various stages of cancer.

Circulating oncomiRs are isolated from most of the body fluids including blood, urine, saliva, tears, semen and breast milk.[12, 21] Circulating oncomiRs remain stable after being subjected to severe settings that would normally degrade other RNAs and, thus, are considered as highly promising disease biomarkers.[12, 21-23] Therefore, development of specific, sensitive and point-of-care detection methodologies for circulating oncomiRs can impact noninvasive or minimally invasive disease screening.

To date there have been several approaches developed for oncomiR detection. For instance, Tripp and coworkers

[a] Department of Chemistry, University at Albany, State University of New York, 1400 Washington Avenue, Albany, New York 12222, United States.
[b] The RNA Institute, University at Albany, State University of New York, 1400 Washington Avenue, Albany, New York 12222, United States.
† Correspondence: M. Yigit*, Email: myigit@albany.edu; Tel: (1) 518-442-3002
Electronic Supplementary Information (ESI) available: Figs. S1-S3 and details of experimental methods are provided. See DOI: 10.1039/x0xx00000x

developed label-free surface enhanced raman spectroscopy SERS and silver nanorod array methodology to detect let-7f with a limit of detection (LOD) equivalent to 28 nM.[24] Bailey and coworkers used silicon photonic microring resonators and detected miR-21, miR-24-1, miR-133b and let-7c extracted from U87 glioblastoma cells and achieved a 0.2 nM detection limit.[25] A chemiluminescence resonance energy transfer platform was developed to detect miR-21 with an LOD of 0.18 nM.[26] Pingarron et al. used an electrochemical biosensor platform to detect endogenous miR-21.[27] Recently, we have used graphene oxide nanosheets for the simultaneous detection of miR-21 and miR-141 from human body fluids using fluorescence spectroscopy and achieved a 1.2 nM detection limit.[22]

DNA nanotechnology using HCR coupled with the plasmonic properties of gold nanoparticles (AuNPs) can be useful for the visual, simple and instrument-free detection of oncomiRs. The colloidal AuNPs (~13 nm sized) exhibit a red color in the dispersed state, but show a purple color when aggregated due to the shift of the surface plasmon band at ~520 nm to longer wavelengths. The change in dispersion states of AuNPs has been investigated for the visual and spectroscopic detection of various molecules.[28, 29]

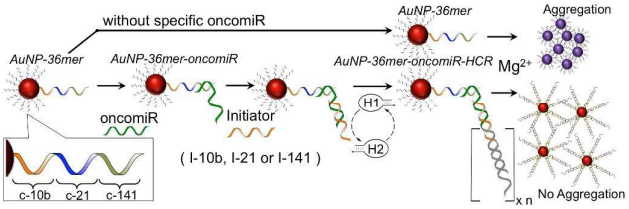

Fig. 1 Schematic illustration of the reprogrammable detection using hybridization chain reaction. The target oncomiR (miR-10b, miR-21 or miR-141) binds partially to the complementary sequences (c-10b, c-21 or c-141) of the capture probe on the AuNP. This provides a sticky end for initiators (I-10b, I-21 or I-141) to bind, which later triggers hybridization chain reaction (HCR). The resulting DNA polymers protect the AuNPs from Mg^{2+} ion induced aggregation, and therefore the original color of the suspension is retained only in the presence of target oncomiR or oncomiRs.

Here, we have employed hybridization chain reaction technology and AuNPs to develop a reprogrammable and highly sensitive methodology for the visual detection of three different circulating oncomiRs dysregulated at different states of breast cancer.[16, 18, 20, 30] One of the most notable features of our technology is that by simply changing the initiator (label-free short single stranded DNA) content of the detection system, while keeping everything else unchanged, we can reprogram our system for the identification of a different oncomiR or groups of oncomiRs, individually or simultaneously.

Fig. 1 depicts the schematic illustration of the programmable and visual detection of three oncomiRs (miR-10b, miR-21 and/or miR-141) using HCR and AuNPs. Briefly, a 36-mer capture-DNA probe is immobilized on AuNPs. The target oncomiR or oncomiRs hybridize with the 36-mer DNA through its complementary c-10b, c-21 or c-141 fragments to form an RNA/DNA heteroduplex with a sticky RNA end. Later, a specific initiator (I-10b, I-21 or I-141, programing component) is added to the *AuNP-36mer-oncomiR* assembly, **Figs. 1** and **S1**. The initiator binds to the sticky end of the oncomiR and forms a second generation of the AuNP assembly with a DNA sticky end, which is able to open up the first hairpin (H1). The opening of the hairpin H1, initiates the opening of H2, and starts the HCR process. As a result, the surface of the AuNP is covered with the orthogonal DNA polymers immobilized through thiolated 36-mer capture probes. This assembly occurs only in the presence of a specific oncomiR or oncomiRs and the correct initiator compositions.

In order to monitor the HCR-induced DNA polymerization on the AuNP surface, and therefore the presence of the target oncomiR strand or strands, the resulting AuNP assembly is treated with Mg^{2+} ions to result in nanoparticle aggregation. The HCR assembly on the gold surface forms and protects the AuNPs from aggregating only in the presence of the programmed target oncomiR or oncomiRs. This phenomenon is observed by a retained red color. Conversely, without the HCR assembly the AuNPs aggregate, which is observed either by an immediate color transition (within seconds) or settlement of a black precipitate and clear suspension after an hour, **Fig. 1**. This system enables us to reprogram the same AuNP template (AuNP-36mer) to identify the presence of a specific oncomiR or a group of oncomiRs simply by changing the initiator composition but nothing else in the system.

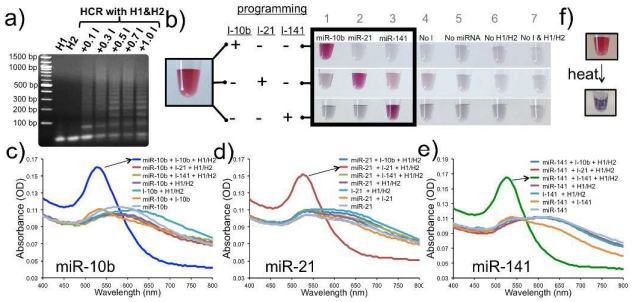

Fig. 2 Identification of individual oncomiR using HCR. (a) DNA polymerization induced by HCR is triggered by various concentrations of initiator strands (I-10b, I-21 or I-141) and demonstrated by gel electrophoresis. (b) Programming the detection of miR-10b, miR-21 or miR-141 using AuNP-36mer, initiator probes (I-10b, I-21 or I-141) and H1/H2 hairpins. Only in the presence of target oncomiR, hairpins and the correct initiator the system allows (b) visual and (c) spectroscopic detection. (d) Melting of the DNA polymers on AuNP surface results in immediate Mg^{2+} ion induced aggregation.

First, in order to characterize the formation of the HCR in the presence of initiators (I-10b, I-21 and/or I-141), gel electrophoresis studies were performed. The gel image in **Fig. 2a** demonstrates the presence of DNA polymerization as a result of HCR, which was triggered by various initiator (I-10b, I-21 or I-141) concentrations. As seen in the gel image, in the absence of initiator, H1 and H2 hairpins show only a single band. On the other hand, when various concentrations of initiators (0.1, 0.3, 0.5, 0.7 and 1.0 fold with respect to hairpin concentrations) were added to H1/H2, large smeared DNA bands were observed in lanes 3 through 7, which suggests an initiator triggered HCR had taken place. The AFM image shows the clusters of DNA polymers in the presence of H1/H2 hairpins and an initiator, **Fig. S2**.

Later, the specificity of this programmable colorimetric approach was tested with three circulating oncomiRs (miR-10b, miR-21, or miR-141) which the AuNP-36mer has binding affinity for through DNA/RNA hybridization. First, we tested our nano-platform with these three oncomiRs individually in the presence or absence of their initiators (I-10b, I-21, or I-141, programming units) and the hairpins H1/H2. In the presence of target oncomiR, the correct specific initiator and the hairpins H1/H2, DNA polymerization on the gold surface protected nanoparticles from Mg^{2+} ion-induced aggregation, which was confirmed visually and spectroscopically (**Figs. 2b-e**). For instance, in the first row of **Fig. 2b**, the AuNP-36mer was programmed for miR-10b detection, but not for miR-21 or miR-141, using initiator-10b (I-10b). As seen only in the presence of miR-10b the nanoparticle suspension retained its colloidal color. On the other hand, other oncomiRs or settings changed the color of the suspension due to the absence of HCR. Later, this same system was re-programmed for miR-21 and miR-141 (second and third rows, respectively) simply by changing the initiator but no other parameter. As seen in **Fig. 2b** only in the presence of miR-21 (second row) and miR-141 (third row) AuNP-36mer retained its colloidal color. The results show that the same AuNP template can be reprogrammed for detection of three different oncomiRs and can be set highly specific for each oncomiR by only replacing the label-free initiator strand in the reaction mixture.

Later, UV-Vis spectroscopy was used to confirm the miR-10b detection by a change in surface plasmon of AuNPs, **Fig. 2c**. Only the nanoparticles with miR-10b and correct inputs for HCR retained the original spectral information whereas other settings resulted in aggregation of the nanoparticles, observed by a shift at 520 nm. Similar results were observed with miR-21 and miR-141 (**Fig. 2d and e**). The results also demonstrate that only with the hairpins (H1/H2), target oncomiR and the correct initiator, which are the necessary components for HCR-induced DNA polymerization, the system is able to detect and discriminate the target oncomiRs. This also indicates that HCR plays the major role in this enzyme-free visual detection approach.

In addition, in order to demonstrate that the nanoparticle stability against Mg^{2+} ions was due to the protection provided by the HCR, the *AuNP-36mer-oncomiR-HCR* assembly was heated to 90 °C to denature the DNA polymers on the surface. An immediate aggregation of AuNPs was observed during the heating process, which confirms that the surface-immobilized DNA polymers had protected the AuNPs from aggregating, **Fig. 2f.** Additionally, the dynamic light scattering data demonstrated that the average size of the nanoparticles increased after HCR, **Fig. S3**. In order to demonstrate the stability of the HCR-induced DNA polymerization on the AuNP surface, the *AuNP-36mer-oncomiR-HCR* was treated with Mg^{2+} ions three hours, one day, two days, one week or two weeks after the formation of HCR products on gold nanoparticles, **Fig. S4**. The results show that the DNA polymers remain stable on the AuNP surface during these time periods.

After demonstrating the visual detection of each oncomiR individually and specifically using the AuNP-36mer, we reprogrammed it for detecting the three oncomiRs simultaneously in groups using the initiator strands with different compositions. By simply incorporating the initiators I-10b and I-21 into the reaction system, the same AuNP-36mer template was reprogrammed for the detection of both miR-10b and miR-21 but not miR-141, (**Figs. 3a and b**). Later, the settings were changed for miR-10b and miR-141 (**Figs. 3a and c**) or miR-21 and miR-141 (**Figs. 3a and d**) by using an initiator cocktail composed of (I-10b and I-141) or (I-21 and I-141), respectively. Finally, the system was reprogrammed for the detection of all three oncomiRs using an initiator cocktail composed of I-10b, I-21 and I-141 (**Figs. 3a and e**). The results demonstrate that the same nano-platform (AuNP-36mer) offered a visual and spectroscopic detection of seven different oncomiR combinations (three individually, three groups of two oncomiRs and one group of all three oncomiRs), the black square in **Fig. 2b** and **Fig 3a**, by only changing the composition of initiators, which are label-free single stranded DNA molecules.

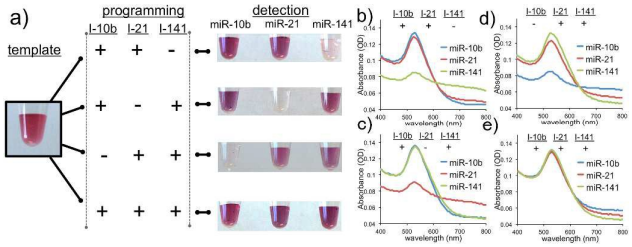

Fig. 3 Identification of oncomiRs simultaneously in various groups using HCR. Reprogramming the (a) visual and (b-e) spectroscopic detection of miR-10b, miR-21 or miR-141 in various groups using AuNP-36mer, H1/H2 hairpins, and various cocktails of reprogramming initiator probes of (b) I-10b and I-21, (c) I-10b and I-141, (d) I-21 and I-141, and (e) I-10b, I-21 and I-141.

Later, the sensitivity of this programmable oncomiR detection methodology was investigated with 0, 20, 40, 100, 200, 500, 1000 and 2000 femtomoles (fmol) of target oncomiRs, **Fig. 4**. Our approach enabled us to detect as little as 20 fmol of miR-21 and miR-10b and 40 fmol of miR-141 visually due to the multiplexed feature of HCR, **Fig. 4 insets**.

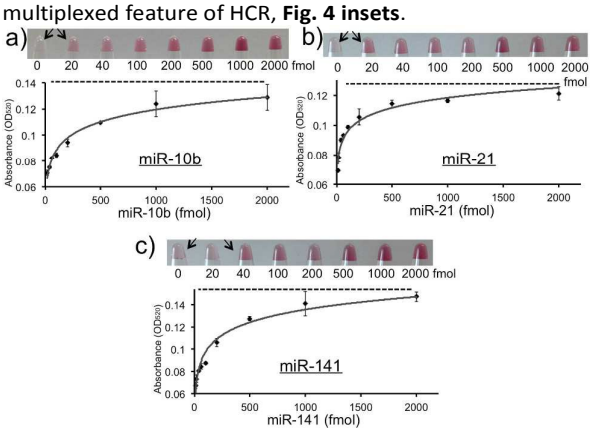

Fig. 4 Detection of different amounts of oncomiRs. Visual and spectroscopic detection of various amounts of (a) miR-10b, (b) miR-21 and (c) miR-141. Arrows show the color difference with as little as 20 fmol of target oncomiR. Dashed lines above the plots show the original absorbance value at 520 nm prior to Mg^{2+} treatment.

In order to demonstrate the identification of the target oncomiRs in an RNA cocktail composed of small and large RNAs, an endogenous total RNA pool isolated from breast cancer cells was used. The experiments were performed with a total RNA pool enriched with exogenous miR-10b, miR-21 or miR-141. The control experiments using endogenous total RNAs without exogenous target oncomiRs resulted in an immediate aggregation of the AuNPs in seconds and settlement after an hour, (**Figs. 5a-c)**. On the other hand, RNA pools with exogenous miR-10b, miR-21 or miR-141 did not change the original color of the suspension at either time points.

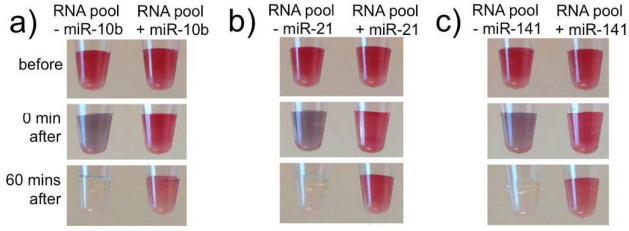

Fig. 5 Detection of target oncomiR in a total RNA pool. Visual identification of exogenous (a) miR-10b, (b) miR-21 and (c) miR-141 in an RNA pool isolated from breast cancer cells.

Finally, in order to demonstrate the detection of endogenous miR-10b, the experiments were performed using the total RNA extracted from a highly metastatic 4T1 breast cancer cell line, which is known to overexpress miR-10b.[17, 31] The results show that the experiments with 50 ng/uL RNA from 4T1 cells prevented AuNPs from aggregating however experiments without endogenous RNAs or with the control cell line resulted in AuNP aggregation after Mg^{2+} treatment, **Fig. S5**.

To conclude, our methodology in this study offers a visual and spectroscopic detection of low amounts of three different circulating oncomiRs, which are found to be dysregulated in different disease states of breast cancer. Combining the multiplexed feature of HCR and the plasmonic properties of AuNPs, we have demonstrated that as little as 20 fmol of a target oncomiR can be identified visually. Furthermore, the outstanding reprogramming property of HCR enabled us to detect three circulating oncomiRs separately or simultaneously in seven different combinations using the same nano-platform. Our system also offered the visual detection of target oncomiRs in an RNA pool containing the endogenous RNAs isolated from the breast cancer cells. In future this system could enable us to determine stage I-III, metastatic and drug-resistant breast cancer from liquid biopsies. We thank BD Biosciences for funding Irfan Khan's appointment at the RNA Institute. We thank Prof. Scott Tenenbaum and Paul Kutscha at the SUNY Polytechnic Institute for the AFM images.

Notes and references

1. E. Crew, M. A. Tessel, S. Rahman, A. Razzak-Jaffar, D. Mott, M. Kamundi, G. Yu, N. Tchah, J. Lee, M. Bellavia and C. J. Zhong, *Anal. Chem.*, 2012, **84**, 26-29.
2. D. Luo, K. A. Carter and J. F. Lovell, *Wiley Interdiscip. Rev. Nanomed. Nanobiotechnol.*, 2015, **7**, 169-188.
3. Y. J. Chen, B. Groves, R. A. Muscat and G. Seelig, *Nat. Nanotechnol.*, 2015, **10**, 748-760.
4. R. M. Dirks and N. A. Pierce, *Proc. Natl. Acad. Sci. U.S.A.*, 2004, **101**, 15275-15278.
5. H. M. Choi, V. A. Beck and N. A. Pierce, *ACS Nano*, 2014, **8**, 4284-4294.
6. H. M. Choi, J. Y. Chang, A. Trinh le, J. E. Padilla, S. E. Fraser and N. A. Pierce, *Nat. Biotechnol.*, 2010, **28**, 1208-1212.
7. Z. Wu, G. Q. Liu, X. L. Yang and J. H. Jiang, *J. Am. Chem. Soc.*, 2015, **137**, 6829-6836.
8. G. Zhu, J. Zheng, E. Song, M. Donovan, K. Zhang, C. Liu and W. Tan, *Proc. Natl. Acad. Sci. U.S.A.*, 2013, **110**, 7998-8003.
9. Y. M. Wang, Z. Wu, S. J. Liu and X. Chu, *Anal. Chem.*, 2015, **87**, 6470-6474.
10. P. Liu, X. Yang, S. Sun, Q. Wang, K. Wang, J. Huang, J. Liu and L. He, *Anal. Chem.*, 2013, **85**, 7689-7695.
11. C. Ma, W. Wang, A. Mulchandani and C. Shi, *Anal. Biochem.*, 2014, **457**, 19-23.
12. P. S. Mitchell, R. K. Parkin, E. M. Kroh, B. R. Fritz, S. K. Wyman, E. L. Pogosova-Agadjanyan, A. Peterson, J. Noteboom, K. C. O'Briant, A. Allen, D. W. Lin, N. Urban, C. W. Drescher, B. S. Knudsen, D. L. Stirewalt, R. Gentleman, R. L. Vessella, P. S. Nelson, D. B. Martin and M. Tewari, *Proc. Natl. Acad. Sci. USA*, 2008, **105**, 10513-10518.
13. A. Lujambio and S. W. Lowe, *Nature*, 2012, **482**, 347-355.
14. C. M. Croce, *N. Engl. J. Med.*, 2008, **358**, 502-511.
15. A. Esquela-Kerscher and F. J. Slack, *Nat. Rev. Cancer*, 2006, **6**, 259-269.
16. L. Ma, J. Teruya-Feldstein and R. A. Weinberg, *Nature*, 2007, **449**, 682-688.
17. M. V. Yigit, S. K. Ghosh, M. Kumar, V. Petkova, A. Kavishwar, A. Moore and Z. Medarova, *Oncogene*, 2013, **32**, 1530-1538.
18. C. Gong, Y. Yao, Y. Wang, B. Liu, W. Wu, J. Chen, F. Su, H. Yao and E. Song, *J. Biol. Chem.*, 2011, **286**, 19127-19137.
19. Z. X. Wang, B. B. Lu, H. Wang, Z. X. Cheng and Y. M. Yin, *Arch. Med. Res.*, 2011, **42**, 281-290.
20. S. Antolin, L. Calvo, M. Blanco-Calvo, M. P. Santiago, M. J. Lorenzo-Patino, M. Haz-Conde, I. Santamarina, A. Figueroa, L. M. Anton-Aparicio and M. Valladares-Ayerbes, *BMC Cancer*, 2015, **15**, 297.
21. A. Sita-Lumsden, D. A. Dart, J. Waxman and C. L. Bevan, *Br. J. Cancer*, 2013, **108**, 1925-1930.
22. M. S. Hizir, M. Balcioglu, M. Rana, N. M. Robertson and M. V. Yigit, *ACS Appl. Mater. Interfaces*, 2014, **6**, 14772-14778.
23. N. M. Robertson and M. V. Yigit, *Wiley Interdiscip. Rev. RNA*, 2014, **5**, 823-833.
24. J. D. Driskell and R. A. Tripp, *Chem. Commun.*, 2010, **46**, 3298-3300.
25. A. J. Qavi and R. C. Bailey, *Angew. Chem. Int. Ed. Engl.*, 2010, **49**, 4608-4611.
26. J. Zhao, X. Jin, M. Vdovenko, L. Zhang, I. Y. Sakharov and S. Zhao, *Chem. Commun.*, 2015, **51**, 11092-11095.
27. S. Campuzano, R. M. Torrente-Rodriguez, E. Lopez-Hernandez, F. Conzuelo, R. Granados, J. M. Sanchez-Puelles and J. M. Pingarron, *Angew. Chem. Int. Ed. Engl.*, 2014, **53**, 6168-6171.
28. J. Liu and Y. Lu, *Angew. Chem. Int. Ed. Engl.*, 2005, **45**, 90-94.
29. N. Bhatt, P. J. Huang, N. Dave and J. Liu, *Langmuir*, 2011, **27**, 6132-6137.
30. M. Chan, C. S. Liaw, S. M. Ji, H. H. Tan, C. Y. Wong, A. A. Thike, P. H. Tan, G. H. Ho and A. S. Lee, *Clin. Cancer Res.*, 2013, **19**, 4477-4487.
31. N. M. Robertson, M. Salih Hizir, M. Balcioglu, R. Wang, M. S. Yavuz, H. Yumak, B. Ozturk, J. Sheng and M. V. Yigit, *Langmuir*, 2015, **31**, 9943-9952.